Avoiding Spectral Efficiency Loss in Unipolar OFDM for Optical Wireless Communication

Dobroslav Tsonev and Harald Haas
Institute for Digital Communications
Li-Fi R&D Centre
The University of Edinburgh
EH9 3JL, Edinburgh, UK
Email: {d.tsonev, h.haas}@ed.ac.uk

***Abstract*—Unipolar orthogonal frequency division multiplexing (U-OFDM) has recently been introduced for intensity modulation and direct detection (IM/DD) systems. The scheme achieves higher power efficiency than the conventional direct-current-biased optical orthogonal frequency division multiplexing (DCO-OFDM) at the expense of half the spectral efficiency for the same M-ary quadrature amplitude modulation (M-QAM) order. This paper presents a modulation approach which doubles the spectral efficiency of U-OFDM and still allows it to achieve better performance in terms of both electrical power and optical power dissipation compared to DCO-OFDM. The simulation results and the theoretical analysis suggest that the performance improvement of the proposed scheme over DCO-OFDM increases with the modulation order. This trend is different from the inherently unipolar state-of-the-art techniques such as U-OFDM, asymmetrically clipped optical orthogonal frequency division multiplexing (ACO-OFDM) and pulse-amplitude-modulated discrete multitone modulation (PAM-DMT). It is typical for these schemes to exhibit a loss in the power efficiency as the spectral efficiency is increased. The novel approach is very promising for the achievement of high data rates in IM/DD systems. To the best of the authors' knowledge, this is the first design of a strictly unipolar orthogonal frequency division multiplexing (OFDM) scheme which requires no biasing and is able to demonstrate significant energy advantage over DCO-OFDM without sacrificing spectral efficiency.**

I. Introduction

Statistical data indicates that demand for wireless communication is growing exponentially. By 2017, data traffic of more than 11 Exabytes per month is expected in mobile networks [1]. Despite the significant technological advances in communication systems, forecasts indicate that meeting the future data rate demands will be challenging. The main reason for this stems from the fact that the radio frequency (RF) spectrum with favourable communication properties is almost completely depleted. A potential solution to the looming spectrum crisis lies in the expansion of wireless communication into new parts of the electromagnetic spectrum such as infrared and visible light wavelengths. Optical wireless communication (OWC) is a major candidate for providing a complementary alternative to RF communication. The optical spectrum features 100s of THz regulation-free bandwidth. Furthermore, optical radiation does not interfere with the operation of sensitive electronic systems and the existing lighting infrastructure could be reused for backhauling. This would simplify the integration of OWC into future heterogeneous wireless networks. Moreover, OWC systems could potentially deliver significant energy savings when successfully combined with existing lighting fixtures.

The foremost candidates for low-cost front-end devices in OWC are commercially available light emitting diodes (LEDs) and photodiodes (PDs). Light emitted by off-the-shelf LEDs is incoherent and, therefore, information can be reliably encoded only in the signal intensity. Phase and amplitude of the light wave cannot be modulated or detected with LEDs and PDs. Hence, an OWC system can be realised only as an intensity modulation and direct detection (IM/DD) system. This limits the set of conventional modulation schemes that can directly be applied from the field of RF communication. Techniques like on-off keying (OOK), pulse-position modulation (PPM), and M-ary pulse-amplitude modulation (M-PAM) are relatively straightforward to implement. With the increase of transmission rates, however, the limited modulation bandwidth of the front-end devices and the limited bandwidth of the OWC channel lead to intersymbol interference (ISI).As a result, orthogonal frequency division multiplexing (OFDM) becomes a more appropriate choice. It enables cost-effective equalisation with single-tap equalisers in the frequency domain as well as adaptive data and energy loading in different frequency bands depending on the channel properties. This results in an optimal use of the communication resources. At medium access control (MAC) level, OFDM provides a straightforward multiple access scheme. It is less straightforward to achieve multiple access in OOK, PPM and M-PAM.

In practice, OFDM is realised by taking an inverse fast Fourier transform (IFFT) of a block of symbols from a conventional modulation scheme such as M-ary quadrature amplitude modulation (M-QAM). This effectively maps the M-QAM symbols to different subcarriers in the frequency domain of the resulting signal. The procedure, however, produces complex-valued time-domain samples, while intensity modulation requires real positive signals. Hence, modifications are required so that the OFDM signal becomes suitable for an IM/DD system. A real signal can be obtained by imposing a Hermitian symmetry in the information block which is passed through the IFFT. The resulting time-domain samples, however, are still bipolar. A number of approaches exist for obtaining a unipolar signal. A straightforward method is to simply add a bias value to all samples, which would make the resulting signal nonnegative. This scheme is called direct-current-biased optical orthogonal frequency division multiplexing (DCO-OFDM). The addition of the direct current (DC) bias increases the energy dissipation of the signal significantly. For example, 4-QAM DCO-OFDM requires a minimum bias which results in a power penalty of about 6 dB, compared to a bipolar OFDM signal. Hence, alternative methods for the generation of unipolar signals have been explored. This has lead to schemes such as asymmetrically clipped optical orthogonal frequency division multiplexing (ACO-OFDM) [2], pulse-amplitude-modulated discrete multitone modulation (PAM-DMT) [3], Unipolar orthogonal frequency division multiplexing (U-OFDM) [4], Flip-OFDM [5], *etc*. All these methods exploit the properties of the fast Fourier transform (FFT) and the properties of the OFDM frame structure in order to realise a unipolar signal without biasing. It is interesting to note that the underlying concepts presented for U-OFDM in [4] and for Flip-OFDM in [5] and [6] are the same. It is also interesting to note that all four approaches achieve the same performance in an additive white Gaussian noise (AWGN) channel [7]. For the same modulation order, the spectral efficiency of each of these four methods is halved when compared to DCO-OFDM. However, the power penalty when compared to a bipolar OFDM signal is only 3 dB for any M-QAM constellation size, which amounts to a significant energy advantage over DCO-OFDM. Improved decoders, which are equivalent in performance, have been developed for ACO-OFDM [8], U-OFDM [4] and Flip-OFDM [6]. Even though, to the best of the authors' knowledge, such an improved decoder is not presented in the literature for PAM-DMT, it would be straightforward to design. The improved decoders make the power efficiency of all four schemes almost equivalent to the case for a bipolar OFDM signal but can only work for a relatively flat communication channel. The real problem, however, stems from the decreased spectral efficiency, which requires M-QAM DCO-OFDM to be compared to M^2-QAM ACO-OFDM/U-OFDM/Flip-OFDM and to M-PAM PAM-DMT in order to keep the achievable data rate equivalent. This causes a substantial loss of energy efficiency compared to DCO-OFDM in all four schemes for a spectral efficiency above 1 bit/s/Hz [9]. Dissanayake *et. al.* have proposed a technique to simultaneously transmit ACO-OFDM and DCO-OFDM in an attempt to close the spectral efficiency gap [10]. However, this method still requires a DC-bias for the generation of DCO-OFDM. The current work proposes an algorithm to simultaneously transmit multiple unipolar data streams which do not require any biasing. As a result, the spectral efficiency loss of U-OFDM is fully-compensated while a significant energy advantage over DCO-OFDM is retained.

The rest of this paper is organized as follows. Section II gives an overview of U-OFDM. Section III presents the modified modulation approach. Section IV makes a performance comparison between the proposed method and DCO-OFDM. Finally, Section V offers concluding remarks.

II. U-OFDM

In U-OFDM [4], after the IFFT operation from the OFDM modulation process, the time-domain signal is subjected to a simple transformation in order to make it unipolar with minimum or no biasing requirements. Each bipolar frame is split into two separate frames, transmitted one after the other. The first one holds the positive time-domain samples and zeros in the places of the negative ones. In the context of this work, this will be referred to as the *positive* frame. The second frame holds the absolute values of the negative samples and zeros in the places of the positive ones. This frame will be referred to as the *negative* frame. This transformation halves the achievable data rate and effectively halves the spectral efficiency which becomes:

$$\eta_{\mathrm{U}} = \frac{\log_2(M)(N_{\mathrm{FFT}}-2)}{4(N_{\mathrm{FFT}}+N_{\mathrm{cp}})} \text{ bits/s/Hz}, \tag{1}$$

as opposed to the spectral efficiency of DCO-OFDM:

$$\eta_{\mathrm{DCO}} = \frac{\log_2(M)(N_{\mathrm{FFT}}-2)}{2(N_{\mathrm{FFT}}+N_{\mathrm{cp}})} \text{ bits/s/Hz}. \tag{2}$$

The factor $\log_2(M)$ indicates the number of bits that are encoded in an M-QAM constellation; N_{FFT} is the FFT size; the factor $(N_{\mathrm{FFT}}-2)/2$ appears because the DC subcarrier and the π-shifted subcarrier are set to zero, and because only half of the subcarriers are modulated uniquely as part of the Hermitian symmetry requirement; N_{cp} is the length of the cyclic prefix.

At the U-OFDM receiver, each original bipolar frame is recovered by subtracting the samples in the *negative* frame from the samples in the *positive* frame. This combines the AWGN at both frames and leads to a signal-to-noise ratio (SNR) penalty of 3 dB when compared to a bipolar OFDM signal. The DC-bias in DCO-OFDM causes a substantial increase in the energy consumption. If the bias is defined as:

$$b_{\mathrm{DC}} = k\sqrt{\mathrm{E}\left\{\mathrm{s}^2(t)\right\}} = k\sigma_{\mathrm{s}}, \tag{3}$$

where $\mathrm{s}(t)$ denotes the bipolar OFDM signal, and $\mathrm{E}\{\cdot\}$ denotes statistical expectation, the energy dissipation of DCO-OFDM increases approximately by:

$$10\log_{10}\left(k^2+1\right)\mathrm{dB} \tag{4}$$

when compared to bipolar OFDM [11]. The minimum biasing requirement of 4-QAM DCO-OFDM, for example, leads to a power penalty of about 6 dB. This penalty increases with the

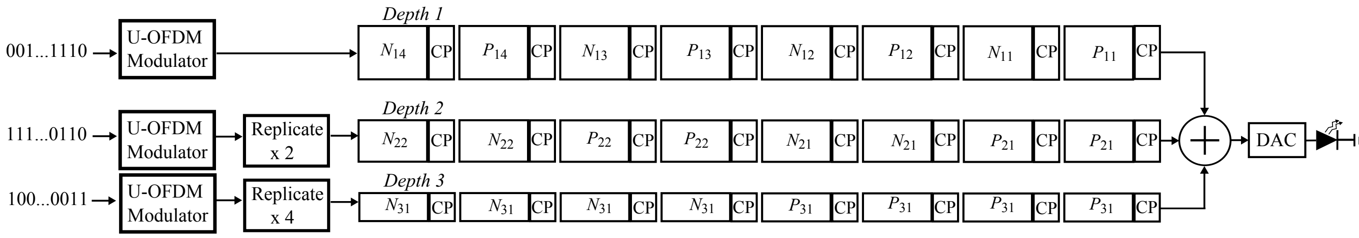

Fig. 1. Illustration of the enhanced U-OFDM concept up to *Depth 3*. CP is the cyclic prefix of each frame. P_{ml} signifies the unipolar frame which holds the positive samples of the lth original bipolar OFDM frame at *Depth* m. N_{ml} indicates the unipolar frame which holds the negative samples of the lth original bipolar OFDM frame at *Depth* m. The illustrated digital-to-analog converter (DAC) includes all necessary operations required for transition from a discrete-time-domain signal to a continuous analog signal. This block includes pulse-shaping and signal amplification. The resulting analog signal drives the LED transmitter.

modulation order. Hence, U-OFDM is more power efficient than DCO-OFDM for the same constellation size. However, as described in Section I, halving of the spectral efficiency means that M-QAM DCO-OFDM should be compared to M^2-QAM U-OFDM for the same spectral efficiency. As a result, U-OFDM very quickly loses its energy efficiency over DCO-OFDM as M increases.

An improved decoder for U-OFDM is presented in [4]. This decoder employs a recombination technique for the *positive* and *negative* frames, which at each position selects the sample with higher amplitude between the two frames. This ideally removes half of the AWGN. However, it is still insufficient to make up for the power penalty which results from the requirement for a higher constellation size compared to DCO-OFDM. Furthermore, this technique is only applicable in relatively flat communication channels where the ISI is negligible. If the ISI is considerable, then this demodulator requires equalisation to be performed in the time domain. In addition, since this method discards half of the U-OFDM samples, the channel attenuation at different frequency subcarriers is not consistent. This renders use of adaptive bit loading techniques difficult. Furthermore, frequency-dependent distortion effects caused by the DC-wandering in electrical circuits as well as by the flickering noise from ambient light sources could become unavoidable and could further aggravate the issues when using this demodulation algorithm.

III. Enhanced U-OFDM

The current paper proposes a modification of U-OFDM which effectively doubles the spectral efficiency. The concept, as illustrated in Fig. 1, allows multiple U-OFDM information streams to be combined in a single time-domain signal used to modulate the LED. A single U-OFDM signal is represented by the information stream, labelled *Depth 1*. A frame labelled with P holds the positive samples of a bipolar OFDM frame and zeros in place of the negative ones. A frame labelled with N holds the absolute values of the negative samples of that same bipolar OFDM frame and zeros in place of the positive ones. The signal at *Depth 1* is generated exactly as described in Section II and in [4]. A second U-OFDM information stream, indicated by *Depth 2*, is superimposed on the first one, and it does not affect the ability of the receiver to recover the transmitted bits as long as the additional stream follows a certain structure. In particular, at *Depth 2*, each U-OFDM frame is replicated and transmitted twice, where the second instance is an exact copy of the first one. Hence, in the figure, the second frame at *Depth 2* is an exact copy of the first one, the fourth frame is an exact copy of the third one, *etc.*., as indicated by their label. Since each frame is transmitted twice in the second stream, the power of each frame instance is scaled by $1/2$. A third stream can be added in the same way as the second one, and the structure requires the U-OFDM frames to be replicated four times now. The power of each frame instance is scaled by $1/4$ in this case. In a similar fashion, additional information streams could be added where each frame would be replicated into 2^{d-1} consecutive frames whose amplitude would be scaled by $1/\sqrt{2^{d-1}}$, where d indicates the depth of the stream.

At the receiver, the modulation stream at *Depth 1* can be demodulated using the standard techniques for U-OFDM. Each *negative* frame is subtracted from each *positive* frame, followed by conventional OFDM demodulation of the obtained bipolar frames. For example, at *Depth 1*, the first bipolar frame is obtained from the operation $P_{11} - N_{11}$, the second one is obtained from the operation $P_{12} - N_{12}$ and so on. The additional streams do not interfere with the successful demodulation because the interference that falls on P_{11} is equivalent to the interference that falls on N_{11} caused by $P_{21} + P_{31}$. Hence, the subtraction operation cancels out both interference terms. The same happens to the interference terms on all subsequent frames at *Depth 1*. Hence, the information at *Depth 1* can be successfully recovered with the conventional U-OFDM demodulator. Once the information bits are demodulated at *Depth 1*, they are remodulated again in order to recover the original U-OFDM signal at *Depth 1*. This signal is then subtracted from the overall received signal, and the result only contains the information streams from *Depth 2* and all subsequent levels. Every two equivalent frames at *Depth 2* are summed. For example, the first and the second frame at *Depth 2* are summed, the third and the fourth frames are summed, *etc.*. Then, the demodulation process continues with the conventional U-OFDM demodulator just like for the information at *Depth 1*. Again, subsequent streams do not interfere because the interference from the subsequent streams is structured in such a way that it is completely removed by the subtraction operation. After the bits are recovered, they are remodulated and the result is subtracted from the remaining received signal. This iterative demodulation procedure continues until the information at all depths is recovered.

The spectral efficiency of the new scheme is the sum of the spectral efficiencies of the information streams at all depths:

$$\eta_{\mathrm{eU}}(D) = \sum_{d=1}^{D} \frac{\eta_{\mathrm{U}}}{2^{d-1}} = \eta_{\mathrm{U}} \sum_{d=1}^{D} \frac{1}{2^{d-1}}, \tag{5}$$

where D is the maximum modulation depth of the scheme, which indicates the total number of streams that are superimposed in the modulation signal. As the maximum modulation depth increases, the spectral efficiency of this enhanced U-OFDM (eU-OFDM) converges to the spectral efficiency of DCO-OFDM:

$$\lim_{D\to\infty} \eta_{\mathrm{eU}}(D) = \eta_{\mathrm{U}} \lim_{D\to\infty} \sum_{d=1}^{D} \frac{1}{2^{d-1}} = 2\eta_{\mathrm{U}} = \eta_{\mathrm{DCO}}. \tag{6}$$

For a maximum modulation depth of D=5, η_{eU} is already 96.8% of η_{DCO}, which means the difference is negligible.

The average power of a U-OFDM signal is $\mathrm{E}\{\sigma_{\mathrm{s}}^2/2\}$, where σ_{s} is the standard deviation of the bipolar OFDM signal, introduced in (3). This result can be quickly deduced from the fact that half of the U-OFDM time-domain samples have the same absolute values as the bipolar OFDM samples and the other half of the U-OFDM samples are set to zero. The average electrical power of the eU-OFDM signal is higher due to the additional information streams. It can be calculated as:

$$\begin{aligned}
P_{\mathrm{elec,eU}}^{\mathrm{avg}} &= \mathrm{E}\{\mathrm{s}_{\mathrm{eU}}^2(t)\} = \mathrm{E}\left\{\left(\sum_{d=1}^{D} \underline{\mathrm{s}}_d(t)\right)^2\right\} \\
&= \sum_{d=1}^{D} \mathrm{E}\left\{\underline{\mathrm{s}}_d^2(t)\right\} + \sum_{d_1=1}^{D} \sum_{\substack{d_2=1 \\ d_1\neq d_2}}^{D} \mathrm{E}\left\{\underline{\mathrm{s}}_{d_1}(t)\right\} \mathrm{E}\left\{\underline{\mathrm{s}}_{d_2}(t)\right\} \\
&= \frac{\sigma_{\mathrm{s}}^2}{2} \sum_{d=1}^{D} \frac{1}{2^{d-1}} + \sum_{d_1=1}^{D} \sum_{\substack{d_2=1 \\ d_1\neq d_2}}^{D} \frac{\phi(0)\sigma_{\mathrm{s}}}{\sqrt{2^{d_1-1}}} \frac{\phi(0)\sigma_{\mathrm{s}}}{\sqrt{2^{d_2-1}}} \\
&= \frac{\sigma_{\mathrm{s}}^2}{2}\left(2 - \frac{1}{2^{D-1}}\right) + \frac{\sigma_{\mathrm{s}}^2}{2} 4\phi^2(0) \sum_{d_1=1}^{D} \sum_{\substack{d_2=1 \\ d_1\neq d_2}}^{D} \frac{1}{\sqrt{2^{d_1+d_2}}},
\end{aligned} \tag{7}$$

where $\mathrm{s}_{\mathrm{eU}}(t)$ is the time-domain eU-OFDM signal, $\underline{\mathrm{s}}_d(t)$ is the time-domain U-OFDM signal at depth d, and $\phi(0)$ is the probability density function (PDF) of the standard normal distribution. In (7), the time-domain expectation of the U-OFDM signal, $\mathrm{E}\left\{\underline{\mathrm{s}}_d(t)\right\} = \phi(0)\sigma_{\mathrm{s}}/\sqrt{2^{d-1}}$, can be quickly derived from the fact that half of the U-OFDM samples follow a Gaussian distribution clipped at zero, and the other half of the samples are set to zero. The truncated Gaussian distribution and its statistical properties are described in more detail in [12]. The number of bits carried by eU-OFDM is $2-1/2^{D-1}$ times more compared to U-OFDM, and, as a consequence, the increase in the required SNR compared to U-OFDM for the same M-QAM constellation size becomes:

$$\alpha = 1 + \frac{4\phi^2(0)}{2 - 1/2^{D-1}} \sum_{d_1=1}^{D} \sum_{\substack{d_2=1 \\ d_1\neq d_2}}^{D} \frac{1}{\sqrt{2^{d_1+d_2}}}. \tag{8}$$

The electrical SNR of the system is defined as:

$$\frac{E_{\mathrm{b,elec}}}{N_{\mathrm{o}}} = \frac{P_{\mathrm{elec,eU}}^{\mathrm{avg}}}{B\eta_{\mathrm{eU}} N_{\mathrm{o}}} = \frac{\mathrm{E}\{\mathrm{s}_{\mathrm{eU}}^2(t)\}}{B\eta_{\mathrm{eU}} N_{\mathrm{o}}}, \tag{9}$$

where B is the communication bandwidth of the system and N_{o} is the power spectral density (PSD) of the AWGN. Given that U-OFDM, decoded by subtraction of the negative frame, performs 3 dB worse than bipolar OFDM, a bound on the performance of eU-OFDM can be easily evaluated theoretically. This is achieved by applying a factor of 2 and a factor of α to the SNR in the formula for calculating the bit error rate (BER) of conventional real M-QAM OFDM. This bound is expected to coincide with the BER curve for the information stream at *Depth 1* of eU-OFDM where distortion is caused only by the AWGN as the inter-stream interference of any subsequent streams can be completely removed by the subtraction operation. The BER of the additional streams is expected to increase with the depth. This occurs because the performance of each stream is affected by the BER of the previous streams. Any errors in the demodulated bits at a given depth translate into imperfections in the iterative cancellation algorithm. This results in overall deterioration of the signal quality at all subsequent information streams. The performances of all streams are expected to converge to the performance of the one at *Depth 1* as the SNR increases. This expected trend is confirmed by the simulation results in Section IV.

In a similar fashion, the average optical power of the eU-OFDM signal can be calculated as:

$$\begin{aligned}
P_{\mathrm{opt,eU}}^{\mathrm{avg}} &= \mathrm{E}\left\{\mathrm{s}_{\mathrm{eU}}(t)\right\} = \mathrm{E}\left\{\sum_{d=1}^{D} \underline{\mathrm{s}}_d(t)\right\} = \sum_{d=1}^{D} \mathrm{E}\left\{\underline{\mathrm{s}}_d(t)\right\} \\
&= \phi(0)\sigma_{\mathrm{s}} \sum_{d=1}^{D} \frac{1}{\sqrt{2^{d-1}}}.
\end{aligned} \tag{10}$$

A closed-form bound can be calculated for the BER performance as a function of the optical SNR. The relationship between electrical SNR and optical SNR can be expressed as the ratio of (7) and (10). This means that for any optical SNR, the equivalent electrical SNR can be obtained, and for

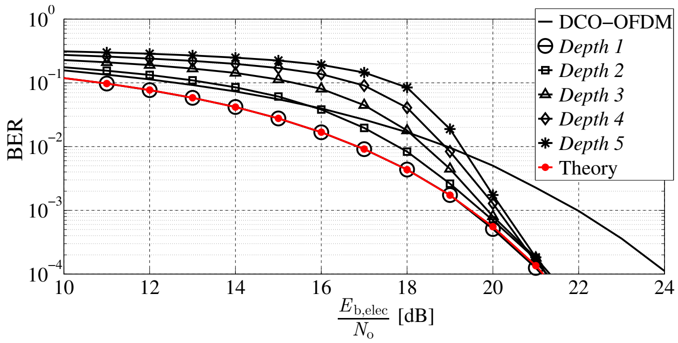

Fig. 2. 16-QAM eU-OFDM performance at different depths as a function of the electrical SNR. The optimum biasing level for 16-QAM DCO-OFDM is estimated at 7.5 dB, as described in (4).

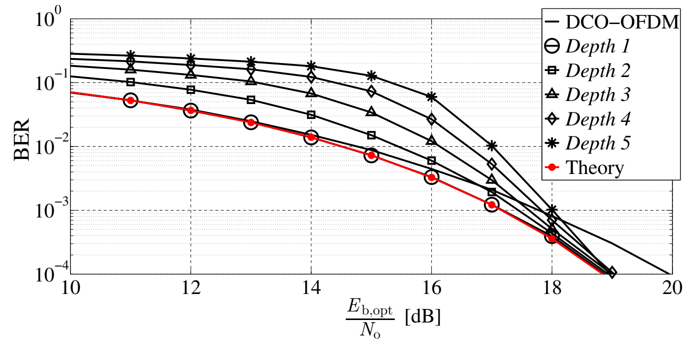

Fig. 3. 16-QAM eU-OFDM performance at different depths as a function of the optical SNR. The optimum biasing level for 16-QAM DCO-OFDM is estimated at 7.5 dB, as described in (4).

the electrical SNR a closed-form bound already exists. The optical SNR of the system is defined as:

$$\frac{E_{\mathrm{b,opt}}}{N_{\mathrm{o}}} = \frac{P_{\mathrm{opt,eU}}^{\mathrm{avg}}}{B\eta_{\mathrm{eU}} N_{\mathrm{o}}} = \frac{\mathrm{E}\left\{s_{\mathrm{eU}}(t)\right\}}{B\eta_{\mathrm{eU}} N_{\mathrm{o}}}. \qquad (11)$$

The calculations presented so far assume an eU-OFDM signal with zero bias. This occurs when at the lowest operational point the LED light intensity output is generally not visible. Then, a zero bias can be assumed for the estimation of the optical efficiency of the system. However, an LED normally requires a minimum bias current at which the device turns on. Therefore, for the calculation of the electrical efficiency, this bias needs to be taken into account. As long as it is small, relative to the span of the information signal, the bias will not introduce significant changes to the energy efficiency of the system. Therefore, in the current study, it is neglected.

IV. Numerical Results

This section compares the performance of DCO-OFDM and eU-OFDM in the context of a linear AWGN channel. The only nonlinear operation considered in this study is clipping of any negative values in the modulation signal. This occurs because an LED is active only for a positive signal. In practice, clipping of the signal from above is also present due to saturation of the optical output power and due to maximum current and optical radiation constraints. This effect is not considered in the current work as it is strongly dependent on the particular device which is used and also dependent on the signal level constraints. The clipping from below, however, is inherent and cannot be avoided in a scheme such as DCO-OFDM unless an impractically large signal bias is introduced. The peak-to-average power ratio (PAPR) of an OFDM signal is quite high and grows linearly with the number of active subcarriers in the frequency domain [13]. Hence, it is very inefficient to use a bias level which can make all possible negative values positive in DCO-OFDM. The novel modulation scheme, eU-OFDM, is strictly positive and so it requires no biasing. In the current study, the maximum modulation depth of eU-OFDM is set to D=5. The performance of the information streams at the different depths is illustrated in Fig. 2. As expected, the stream at *Depth 1* performs best and its BER curve matches exactly the theoretical bound described in Section III. All subsequent streams converge to the performance of the first one as the SNR increases. The same behaviour is depicted in Fig. 3 where the performance of eU-OFDM is illustrated as a function of the optical SNR.

The average BER of the information at all depths is compared against the BER of DCO-OFDM for different M-QAM constellation sizes. Fig. 4 presents the results as a function of the electrical SNR. At BER=10^{-4}, the performance improvement of eU-OFDM over DCO-OFDM starts at 1 dB for M=4 and increases to about 5 dB for M=256. The bias levels for the different realisations of DCO-OFDM are optimised through Monte Carlo simulations, in agreement with previous works such as [12], [14]. This means that adding less bias would lead to more clipping and, hence, to higher BER values for a given SNR, while adding more bias would lead to higher SNR levels without actually reducing the BER. The bias level in each case is indicated as the estimated SNR increase in dB compared to the case for a bipolar OFDM signal as described in (4). It is interesting to note that, for a depth of D=5, the factor for the SNR increase of eU-OFDM, described in (8), is α=1.96, which translates in an SNR penalty of less than 6 dB, compared to the real bipolar OFDM signal. This SNR penalty is constant for all values of the constellation size M. Therefore, it is easy to explain and quantify the increasing energy advantage of eU-OFDM over DCO-OFDM with the increase of the M-QAM modulation order. Fig. 5 illustrates the performance difference between eU-OFDM and DCO-OFDM for different modulation orders in terms of the BER as a function of the optical SNR. For M=4, the two schemes seem to perform equivalently at BER=10^{-4}. As the constellation size increases, the increasing biasing requirement of DCO-OFDM causes eU-OFDM to become more efficient. The savings in terms of optical power reach about 2 dB for 256-QAM.

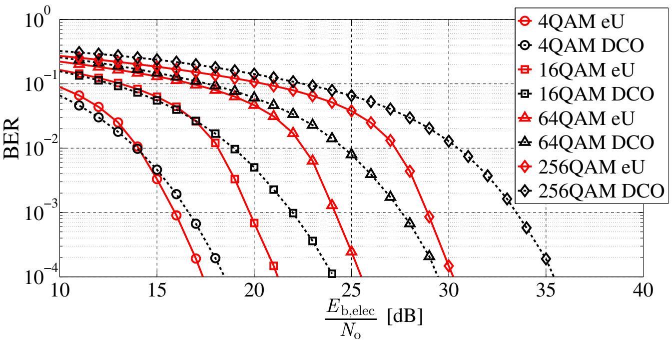

Fig. 4. eU-OFDM performance vs. DCO-OFDM performance for different M-QAM constellation size as a function of the electrical SNR. Optimum biasing levels for 4-QAM, 16-QAM, 64-QAM, and 256-QAM DCO-OFDM are estimated at respectively 6 dB, 7.5 dB, 9.5 dB, and 11 dB, as described in (4).

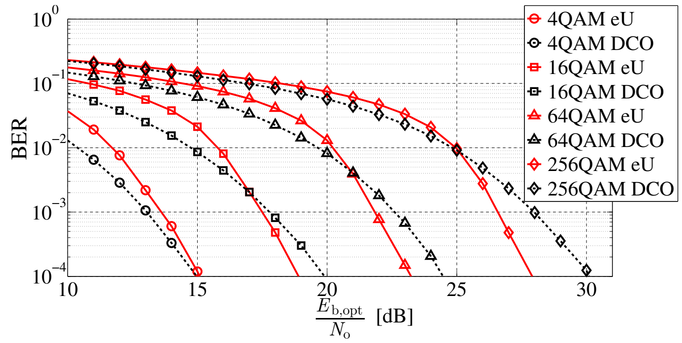

Fig. 5. eU-OFDM performance vs. DCO-OFDM performance for different M-QAM modulation order as a function of the optical SNR. According to (4), optimum biasing levels for 4-QAM, 16-QAM, 64-QAM, and 256-QAM DCO-OFDM are set at 6 dB, 7.5 dB, 9.5 dB, and 11 dB, respectively.

V. Conclusion

A novel approach for increasing the spectral efficiency of U-OFDM has been presented in this paper. It allows U-OFDM to approach the spectral efficiency of DCO-OFDM without the need to introduce any form of biasing, apart from the practical minimum around the turn-on voltage, and, as a consequence, the new scheme avoids energy efficiency losses due to LED biasing. The new method achieves significant improvements in terms of both electrical power dissipation and optical power dissipation. The better energy efficiency of the scheme comes at the cost of increased computational complexity in the modulation and demodulation procedures. At the same time, the design complexity of the analog circuitry is reduced, compared to DCO-OFDM, since the biasing level needs to be optimised only once for any signal strength and any constellation size.

The other two types of unipolar OFDM - ACO-OFDM and PAM-DMT - include a special structure within their time-domain frame which allows well-structured interference terms to be orthogonal to the useful information. As a consequence, the authors believe that the currently presented concept could be extended to those schemes as well. Further work on the subject may include a more detailed evaluation of ACO-OFDM and PAM-DMT. In addition, a performance analysis of eU-OFDM in the presence of nonlinear distortion, resulting from the electrical-to-optical characteristics of an LED, will also be conducted.

The other two types of unipolar OFDM - ACO-OFDM and PAM-DMT - include a special structure within their time-domain frame which allows well-structured interference terms to be orthogonal to the useful information. As a consequence, the authors believe that the currently .

Acknowledgement

We gratefully acknowledge support for this work from the UK Engineering and Physical Sciences Research Council (EPSRC) under grant EP/I013539/1.

References

[1] Cisco Visual Networking Index, “Global Mobile Data Traffic Forecast Update, 2012-2017,” CISCO, White Paper, Feb. 2013. [Online]. Available: http://www.cisco.com/en/US/solutions/collateral/ns341/ns525/ns537/ns705/ns827/white_paper_c11-481360.pdf

[2] J. Armstrong and A. Lowery, “Power Efficient Optical OFDM,” *Electronics Letters*, vol. 42, no. 6, pp. 370–372, Mar. 16, 2006.

[3] S. C. J. Lee, S. Randel, F. Breyer, and A. M. J. Koonen, “PAM-DMT for Intensity-Modulated and Direct-Detection Optical Communication Systems,” *IEEE Photonics Technology Letters*, vol. 21, no. 23, pp. 1749–1751, Dec. 2009.

[4] D. Tsonev, S. Sinanović, and H. Haas, “Novel Unipolar Orthogonal Frequency Division Multiplexing (U-OFDM) for Optical Wireless,” in *Proc. of the Vehicular Technology Conference (VTC Spring)*, IEEE. Yokohama, Japan: IEEE, May 6–9 2012.

[5] N. Fernando, Y. Hong, and E. Viterbo, “Flip-OFDM for Optical Wireless Communications,” in *Information Theory Workshop (ITW)*, IEEE. Paraty, Brazil: IEEE, Oct., 16–20 2011, pp. 5–9.

[6] ——, “Flip-OFDM for Unipolar Communication Systems,” *IEEE Transactions on Communications*, vol. 60, no. 12, pp. 3726–3733, Dec. 2012.

[7] D. Tsonev, S. Sinanovic, and H. Haas, “Complete Modeling of Nonlinear Distortion in OFDM-Based Optical Wireless Communication,” *IEEE Journal of Lightwave Technology*, vol. 31, no. 18, pp. 3064–3076, Sep. 15 2013.

[8] K. Asadzadeh, A. Dabbo, and S. Hranilovic, “Receiver Design for Asymmetrically Clipped Optical OFDM,” in *GLOBECOM Workshops (GC Wkshps)*. Houston, TX, USA: IEEE, Dec., 5–9 2011, pp. 777–781.

[9] S. Dimitrov, S. Sinanovic, and H. Haas, “A Comparison of OFDM-based Modulation Schemes for OWC with Clipping Distortion,” in *GLOBECOM Workshops (GC Wkshps)*, Houston, Texas, USA, 5–9 Dec. 2011.

[10] S. Dissanayake, K. Panta, and J. Armstrong, “A Novel Technique to Simultaneously Transmit ACO-OFDM and DCO-OFDM in IM/DD Systems,” in *IEEE GLOBECOM Workshops (GC Wkshps)*. Houston, TX, USA: IEEE, Dec. 5–9 2011, pp. 782–786.

[11] J. Armstrong and B. J. C. Schmidt, “Comparison of Asymmetrically Clipped Optical OFDM and DC-Biased Optical OFDM in AWGN,” *IEEE Communications Letters*, vol. 12, no. 5, pp. 343–345, May 2008.

[12] S. Dimitrov, S. Sinanovic, and H. Haas, “Clipping Noise in OFDM-based Optical Wireless Communication Systems,” *IEEE Transactions on Communications (IEEE TCOM)*, vol. 60, no. 4, pp. 1072–1081, Apr. 2012.

[13] D. Tsonev, S. Sinanović, and H. Haas, “Enhanced Subcarrier Index Modulation (SIM) OFDM,” in *GLOBECOM Workshops (GC Wkshps)*, IEEE. Houston, Texas, USA: IEEE, Dec. 5–9, 2011.

[14] S. Dimitrov and H. Haas, “Information Rate of OFDM-Based Optical Wireless Communication Systems With Nonlinear Distortion,” vol. 31, no. 6, pp. 918 – 929, Mar. 15 2013.